The Crystalline Structures of Carboxylic Acid Monolayers Adsorbed on Graphite

A. K. Bickerstaffe, N. P. Cheah, S. M. Clarke,* J. E. Parker, A. Perdigon, and L. Messe

BP Institute and Department of Chemistry, University of Cambridge, Madingley Rise, MadingleyRoad, Cambridge, CB3 0HE, U.K.

A. Inaba

Research Center for Molecular Thermodynamics, Graduate School of Science, Osaka University, Toyonaka, Osaka 560-0043, Japan

Received: August 25, 2005; In Final Form: January 18, 2006

X-ray and neutron diffraction have been used to investigate the formation of solid crystalline monolayers of all of the linear carboxylic acids from C_6 to C_{14} at submonolayer coverage and from C_8 to C_{14} at multilayer coverages, and to characterize their structures. X-rays and neutrons highlight different aspects of the monolayer structures, and their combination is therefore important in structural determination. For all of the acids with an odd number of carbon atoms, the unit cell is rectangular of plane group pgg containing four molecules. The members of the homologous series with an even number of carbon atoms have an oblique unit cell with two molecules per unit cell and plane group p2. This odd−even variation in crystal structure provides an explanation for the odd−even variation observed in monolayer melting points and mixing behavior. In all cases, the molecules are arranged in strongly hydrogen-bonded dimers with their extended axes parallel to the surface and the plane of the carbon skeleton essentially parallel to the graphite surface. The monolayer crystal structures have unit cell dimensions similar to certain close-packed planes of the bulk crystals, but the molecular arrangements are different. There is a 1−3% compression on increasing the coverage over a monolayer.

Introduction

Recent work continues to highlight the importance of detailed crystal structures to understand the behavior of adsorbed monolayers in a wide variety of situations. For example, the mixing behavior of adsorbed alkanes and alcohols can be understood in terms of the similarities of the crystal structures of the pure monolayers, and the adsorbed layer structure can be key to the wetting of a surface and templating of bulk crystal growth.[1−4] Odd−even melting variation in monolayer points can also be explained in terms of subtle crystallographic differences.[5,6] In this work, we report the monolayer crystal structures of relatively short (C_6–C_{14}) linear carboxylic acids adsorbed on graphite at submonolayer and multilayer coverages. Carboxylic acids are an industrially important class of adsorbates, being a major component of greases and lubricants.[7]

The formation of ordered adsorbed monolayers of alkanes, alcohols, and acids was first indicated using delicate dilatometry and calorimetry studies.[8,9] There are now fairly extensive X-ray and neutron diffraction investigations of alkanes and alcohols[5,6,10−14] adsorbed on graphite, which also indicate well-ordered monolayers with a rich complexity of behavior. This present work is the first comprehensive combined X-ray and neutron scattering study of adsorbed layers of saturated fatty acids on graphite. STM has also been used to investigate a wide variety of physisorbed monolayers of simple alkyl species on graphite,[15] including some carboxylic acids adsorbed from phenyl octane solution. Myristic (C_{14}), palmitic (C_{16}), heptadecanoic (C_{17}),[16] stearic (C_{18}),[17] nonadecanoic (C_{19}),[16] and arachidic[18] (C_{20}) acids are reported to show well-developed monolayers with strongly hydrogen-bonded dimers. The majority of acids studied have even numbers of carbon atoms and are found to form slightly oblique unit cells with plane group p2 that exhibit a positional correlation with the underlying graphite. The alkyl chains interdigitate, and there is a superstructure in the direction perpendicular to the chains with a repeat distance of four or five molecules. The only odd members to have been studied, heptadecanoic[16] (C_{17}) and nonadecanoic (C_{19}), are reported to exhibit a different pgg symmetry and a rectangular unit cell. Behenic (C_{22}) acid has been reported to show two different monolayer structures with and without interdigitated alkyl chains,[19] both commensurate with the underlying graphite, when formed by a Langmuir−Blodgett technique. STM measurements of the side to side separation between adjacent alkyl chains in monolayers of saturated acids have been reported to be 0.48,[18] 0.426,[19] 0.462, or 0.497 nm.[20] Rabe[21] et al. who studied stearic (C_{18}), arachidic (C_{20}), and tetracosanoic (C_{24}) acids conclude that the mismatch between the side by side separation of alkyl chains and the graphite lattice parameters is approximately 10%. The vast majority of reports indicate that the long axis of the fatty acids is parallel to the graphite. However, there are indications that fatty acids can be upright on a graphite surface when present as metal salts.[19] Interestingly, studies of an unsaturated fatty acid, elaidic acid,[18] have reported molecular structures similar to those of the saturated fatty acids. Interpretation of STM data is rather complex, and the sweeping of the STM probe can perturb the delicate physisorbed structures trying to be imaged. The diffraction techniques used in this present work provide an important noninvasive probe of monolayer structure, providing

* Corresponding author. E-mail: stuart@bpi.cam.ac.uk.

10.1021/jp054798q CCC: $33.50
Published on Web 02/24/2006

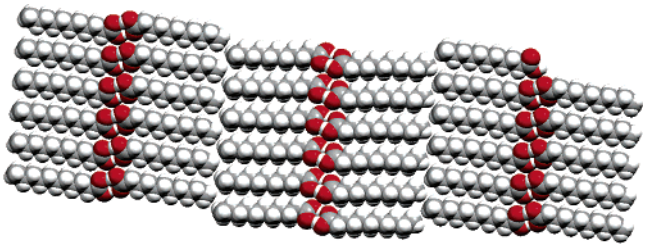

Figure 1. Illustration of layers of hydrogen-bonded molecular dimers that make up the bulk crystal of undecanoic acid (C_{11}).

important independent structural information to compare with STM work. In addition, the structural details of the important hydrogen-bonding groups can be probed by diffraction when they are essentially invisible with STM. The focus of our study here will be shorter homologues than were previously studied by STM.

The bulk crystal structures of carboxylic acids have been reported recently.[22] The closely packed planes in these bulk crystals indicate molecular layers with acid dimers lying parallel to each other in the plane of the layer, as illustrated in Figure 1. These layers are clearly candidates for the adsorbed monolayer structures. The high dimerization energies are expected to dominate the relatively weak physisorption energies in the monolayer structures. Monolayers of chemisorbed alkanethiols on substrates such as silver and gold[23−25] also show ordered monolayers but with relatively higher adsorbate−substrate interaction energies. Alkanes directly adsorbed onto gold have also been investigated using helium atom scattering and are reported to form two phases.[25] The surface corrugation on gold is found to be stronger than the chain−chain interactions energies of the dodecane molecules.

In this work, we present X-ray and neutron diffraction data that confirm the formation of solid monolayers and provide a detailed structural analysis of the solid monolayers formed by all of the members of the homologous series of linear carboxylic acids from hexanoic (C_6) to tetradecanoic (C_{14}). We extend the species of fatty acids investigated previously to shorter homologues including both odd and even members of the series. The work here also demonstrates significant coverage-dependent changes in the monolayer structures not previously reported for fatty acids on graphite. Here, we study adsorption of the pure materials from their liquids. Solvents have been reported to change the monolayer structures,[26] the surface composition, and molecular dynamics,[27] and can be incorporated into the layer itself.[28]

Experimental Section

The apparatus and procedures used to obtain the neutron diffraction patterns from adsorbed layers have been described in detail elsewhere.[29] The instrument used here was D20 at the Institut Laue-Langevin, Grenoble.[29] The temperature was controlled using a standard ILL cryo-furnace. For these neutron experiments, disks of graphite (either clean or dosed with the appropriate acid), approximately 20 mm in diameter, are stacked in an aluminum cylindrical can, to a height of approximately 80 mm. The can is sealed under helium in a glovebag with indium wire. For temperatures above the melting point of indium, spring-energized silver-coated compression rings were used to seal the cans. The cans were attached to the end of a standard orange helium cryostat center stick and placed in the cryostat. On the instrument D20, the sample was irradiated with neutrons of a fixed wavelength 0.242 nm in a beam approximately 18 mm wide and 50 mm tall. The scattered neutrons are collected on a 1600 cell 1D banana multidetector in the horizontal plane.

TABLE 1: Coverages Used for the Neutron Diffraction Measurements at Low ("Submonolayer") and High Coverages ("Multilayer"), and the Coverages for the X-ray Measurements at Low Coverage

acid	X-ray coverage	neutron coverage	
		submonolayer	multilayer
C_6	0.51	0.80	n/a
C_7	0.51	0.80	n/a
C_8	0.50	0.84	3.14
C_9	0.51	0.84	3.12
C_{10}	0.48	0.92	3.40
C_{11}	0.49	0.94	5.96
C_{12}	0.48	0.92	5.85
C_{13}	0.49	0.93	3.51
C_{14}	0.48	0.92	3.47

X-ray experiments were performed on a Rigaku device in symmetrical transmission geometry at the University of Osaka, Japan, as described previously, with an incident wavelength of 0.154 nm and a closed cycle refrigerator.[30] For the X-ray experiments, a single sheet of graphite is irradiated by copper Kα radiation. The device uses a symmetrical transmission geometry with a single scanning detector and a $\theta/2\theta$ sample and detector movement to maintain the momentum transfer in the plane of the graphite sample.

Scattering from crystalline two-dimensional adsorbed layers gives rise to characteristic diffraction peaks[31,32] with a sawtooth line shape. In a fashion similar to 3D crystallography, solution of monolayer diffraction patterns is undertaken by consideration of close packing arguments and the possible plane groups available to molecules with particular point groups.[33] The diffraction pattern from an adsorbed monolayer is obtained by subtraction of the scattering from the substrate alone from that of the substrate and adsorbed material together. For the neutron scattering experiments, deuterated acids were used to minimize any incoherent scattering background that would have arisen from protonated samples. These were obtained from the group of Dr. R. K. Thomas at the University of Oxford. In this work, the single OH proton on the acids group was not deuterated. The combination of X-ray and neutron scattering is extremely important in the structural solution, as illustrated below. Both approaches are readily used at low, submonolayer coverage. However, at high coverages, where there is significantly more adsorbate to penetrate, only neutrons, which have relatively good transmission, can be easily used.

The adsorbent used for both the X-ray and the neutron studies was recompressed exfoliated graphite Papyex (Le Carbone Lorraine). This material is prepared by intercalation between the graphite sheets followed by rapid heating to separate the sheets exposing a very large area of the graphite basal plane. The powder formed by this exfoliation procedure is then lightly recompressed to hold the individual crystallites into a single mass while retaining a high specific surface area. This recompression gives preferred orientation to the graphite crystallite powder, which can be used to optimize the scattering geometery. Each sample was characterized by adsorption of nitrogen. The material used for the neutron studies had a specific surface area of 30.4 $m^2\ g^{-1}$, and that for the X-ray experiment had a specific area of 16.6 $m^2\ g^{-1}$. The graphite was outgassed under vacuum at 350 °C before known quantities of adsorbate were added and annealed in glassware under reduced pressure at 200 °C. Given the relatively large quantities of graphite and its high specific surface area, we are able to expose the substrate to well-defined amounts of adsorbate. We express coverage in terms of the approximate number of equivalent monolayers adsorbed, esti-

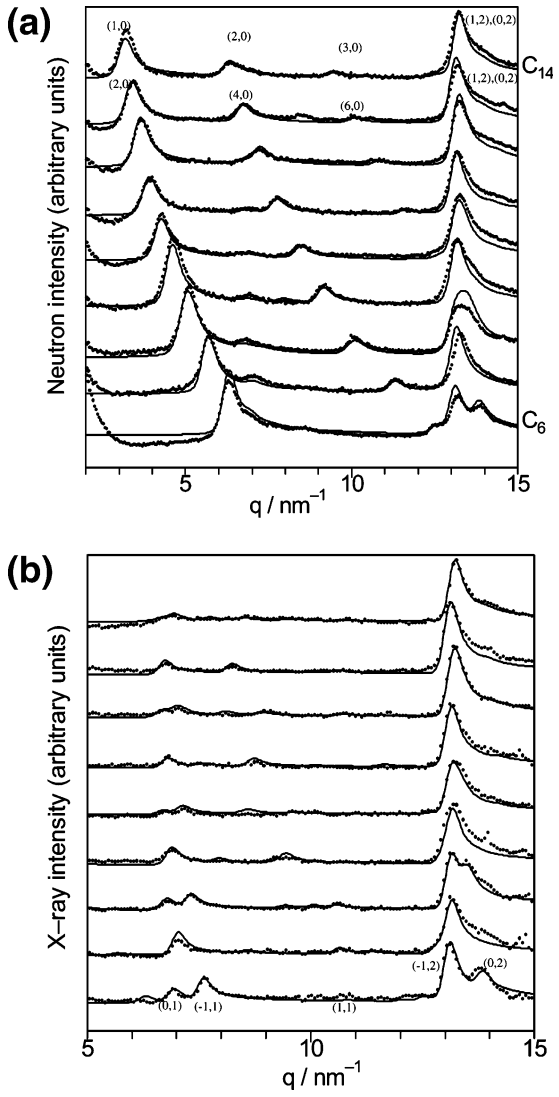

Figure 2. (a) Experimental (crosses) and calculated (lines) neutron diffraction patterns from 0.9 monolayers of hexanoic (C_6) (bottom), heptanoic (C_7), octanoic (C_8), nonanoic (C_9), decanoic (C_{10}), undecanoic (C_{11}), dodecanonoic (C_{12}), tridecanoic (C_{13}) and tetradecanoic (C_{14}) (top) acids adsorbed on graphite. (b) Experimental (crosses) and calculated (lines) X-ray diffraction patterns from 0.9 monolayers of hexanoic (C_6) (bottom), heptanoic (C_7), octanoic (C_8), nonanoic (C_9), decanoic (C_{10}), undecanoic (C_{11}), dodecanonoic (C_{12}), tridecanoic (C_{13}), and tetradecanoic (C_{14}) (top) acids adsorbed on graphite. The indexing of representative principal reflections has been indicated.

mated from the area per molecule, taken from the work of Groszek,[34] and the specific surface area of the graphite. The results of this work allow the true area per molecule to be calculated from the molecular structure and unit cell we obtain. The coverage determined in this way is given in Table 1 for all of the neutron and X-ray measurements. Measurements at submonolayer coverages were made at approximately 10 K for the X-ray measurements and approximately 100 K for the neutron experiments. The high coverage patterns are collected at a different temperature for each acid, in a temperature region where the adsorbed monolayer is solid but the rest of the adsorbate is liquid. Hence, at high coverages, we examine the solid monolayer that coexists with the bulk liquid adsorbate.

Results

Figure 2a presents the experimental neutron scattering patterns from all of the carboxylic acids from hexanoic (C_6) to tetradecanoic (C_{14}) adsorbed on graphite at submonolayer coverages. The graphite background has been subtracted in preparing these figures, and intense small angle scattering from the external form of the graphite crystallites has been removed with a Q^{-4} Porod-type correction.

The peaks in Figure 2a are then the diffraction from the adsorbed monolayers. The peaks have the characteristic asymmetric line shape expected from two-dimensional layers.[31,32] The line profiles depend on several factors including the size of the 2D crystallites, the extent of positional order in the layer, and the degree of preferred orientation.[31,32]

Figure 2b presents the experimental X-ray scattering patterns from monolayers of all of the linear carboxylic acids from hexanoic (C_6) to tetradecanoic (C_{14}) adsorbed on graphite. Data in these figures show X-ray and neutron data as a function of q, the momentum transfer, given by $q = 4\pi \sin(\theta)/\lambda$, where θ is one-half the scattering angle and λ is the radiation wavelength.

A comparison of X-ray and neutron data clearly indicates that, while some reflections appear in both patterns, some appear only in one. Importantly it is noted that the lowest index reflection in the neutron data is not observed in the X-ray data. This arises from the significantly different appearance of the different ends of the molecules when observed by X-rays and neutrons. The X-rays are dominated by the carbon and oxygen atoms in the structure, which have similar electron densities. The pronounced difference in the numbers of protons at each end of the molecules is only reflected in the neutron patterns, which strongly differentiate between hydrogen and deuterium (e.g., neutrons can readily distinguish −OH from −OD). Hence, the X-rays crudely see an essentially symmetric molecule, while the neutrons readily distinguish the two ends of the molecules and reveal the full symmetry of the layer.

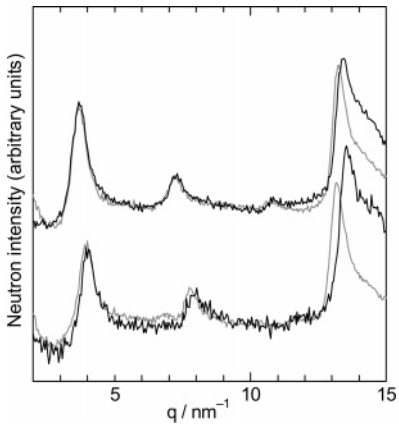

Figure 3. Representative neutron diffraction patterns from the high and low coverage monolayers of undecanoic (C_{11}) and dodecanoic acid (C_{12}) adsorbed on graphite (thick lines, high coverage; thin lines, low coverage). Notice the small shifts in peak positions corresponding to compression in the solids layers on increasing the coverage.

Figure 3 presents representative examples of the neutron diffraction data from the monolayers of the adsorbed acids at higher, multilayer coverages for C_{11} and C_{12} homologues. Scattering from the bare graphite and the liquid adsorbate has been removed in preparing this figure. The patterns at these higher coverages are very similar to those at submonolayer coverage in Figure 2, apart from small but significant shifts in the peak positions as discussed below. Figure 3 clearly indicates that these acids adsorb solid monolayers that coexist with the liquid adsorbate.

In summary, Figures 2 and 3 confirm that all of these simple linear carboxylic acids form solid ordered monolayers on

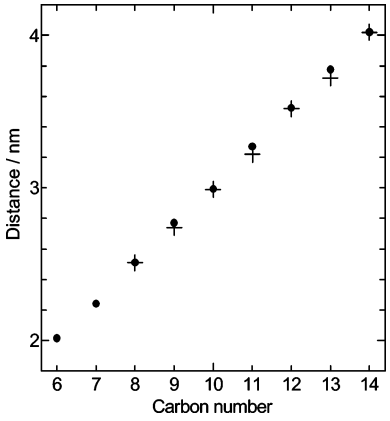

Figure 4. Variation with alkyl chain length in the distance corresponding to the lowest order peak position. Submonolayer (●) and multilayer (+). The estimated errors are submonolayer, 0.01 nm, and multilayer, 0.05 nm.

graphite at submonolayer and multilayer coverages when they coexist with the liquid.

Structural Analysis

Because of the limited number of reflections usually accessible in patterns from 2D layers, only a limited number of structural parameters can realistically be extracted from an analysis. Here, we have adopted the usual convention of solving the patterns with the most highly constrained parameter set possible; it is always easier to fit an experimental pattern by adding more variables. Hence, we have used a high-symmetry rectangular unit cell before moving to less symmetric and then oblique unit cells if solutions cannot be found. Molecular bond lengths and angles and the dimensions of the hydrogen bond have been taken to be those observed in the bulk.[22] The diffraction pattern for each trial structure was calculated as described previously using the Warren 2D line shape[32] corrected for preferred graphite orientation.[31]

In the fitting the Debye−Waller term was calculated using a fixed value of the mean square displacement, u^2, of 2.0×10^{-3} nm^2. The instrumental resolution of the diffractometers was determined using high-quality powdered samples as a reference.

General Observations. The lowest angle reflections in all of the neutron patterns of Figure 2a correspond to the relatively longest *d* spacings in the unit cell. These spacings confirm that the molecules are adsorbed with their long molecular axis parallel to the graphite surface, as reported in STM studies of acids adsorbed from solution on graphite[16,17] and in contrast to the adsorption of fatty acids at the air/water interface and fatty acids salts adsorbed on graphite from the liquid where they adsorb with their long axis essentially perpendicular to the surface.[19]

Figure 4 presents the variation in the position of the lowest order peak with alkyl length for the low coverage, submonolayer structures. The figure shows that there is an essentially linear increase in the "*a*" parameter with alkyl chain length for both odd and even members at low coverage. In contrast, the large peaks at $q = 13.0$ nm^{-1} in the neutron patterns of Figure 2a do not change significantly with increasing alkyl chain length. This feature suggests that, although the unit cell expands significantly in the *a*-direction with longer molecules, the side-to-side packing of molecules is less variable.

At higher coverages, there is a weak (approximately 2%) shift in the "*a*" parameters to lower values for the layers of the odd homologues, giving unit cell parameters of both "odd" and "even" homologues that are similar to the bulk lattice parameters in the direction of the long axis of the molecules. It should be noted here that, although the lattice parameters of the high coverage layers resemble those in the bulk, the molecular orientation in the unit cell is different. The "*b*" parameter of the adsorbed layers also changes on increasing the coverage. In all cases, for both odd and even homologues, there is a shift to higher scattering angle, corresponding to a compression in the adsorbed layer of approximately 1−3%. For example, the "*b*" parameter for undecanoic acid is 0.972 nm at low coverages and 0.946 nm at high coverages. Similar compressions on increasing the coverage are seen in adsorbed alkanes on graphite, where uniaxially commensurate low-coverage monolayers compress to form fully commensurate layers.[5,6] All of the high coverage lattices have very similar "*b*" parameters. The closest commensurate distance is 4 times the graphite lattice periodicity a_g, where a_g is 0.246 nm and $4a_g$ is 0.984 nm. Interestingly, it is the low coverage phase that is closest to this value, and heptanoic acid the closest of the acids. However, it is important to indicate that in diffraction studies such as these we cannot positively identify the formation of a commensurate monolayer, but rather we can only identify potential coincidences between lattice parameters of the monolayer and the underlying graphite periodicity.

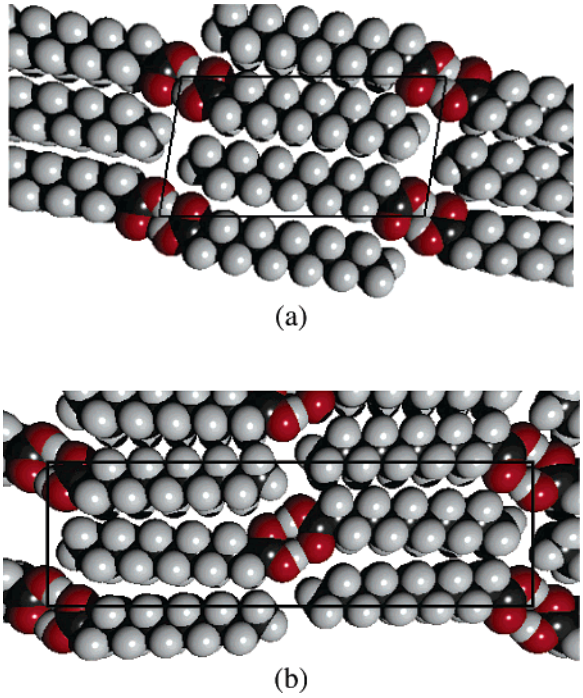

Figure 5. Schematic illustrations of the experimentally determined monolayer crystal structures for (a) dodecanoic acid (C_{12}) and (b) undecanoic acid (C_{11}).

Crystallographic Analysis. It was found that good fits to the experimentally determined peak positions of Figure 2a and b were obtained with the structures illustrated schematically in Figure 5. In all cases, identical monolayer structures were used to provide good fits to both the X-ray and the neutron patterns. Given the different symmetry apparent in these patterns, this represents a significant restraint on the possible structural solutions. The experimentally determined cell parameters are given in Table 2, and the calculated diffraction patterns are shown in Figure 2a and b by solid lines. The fractional coordinates for the repeating motif in the unit cell of undecanoic acid are given in Table 3. We discuss the accuracy of the determination of these structures below.

TABLE 2: Experimentally Determined Structural Parameters for the Adsorbed Monolayers of the Carboxylic Acids[a]

acid	*a*/nm	*b*/nm	υ/deg	tilt/deg
6	1.07	0.97	110	14
7	2.24	0.98	90	3
8	1.30	0.97	105	11
9	2.77	0.98	90	3
10	1.53	0.97	102	11
11	3.27	0.97	90	2
12	1.79	0.96	100	9
13	3.78	0.97	90	1
14	2.03	0.96	98	8

[a] *a*, *b*, and υ are the unit cell lattice parameters, and "tilt" is the angle between the molecular long axis and the long direction of the unit cell. The uncertainties in the lattice parameters are estimated to be 0.01 nm in *a* and 0.002 nm in *b*. The uncertainty in the tilt angle is estimated at 3°.

TABLE 3: Fractional Coordinates for a Single Repeating Motif for the Submonolayer Structure of C_{11}

	fractional coordinates	
atom	*x*	*y*
O1	0.0191	−0.1677
O2	0.0498	0.0350
H	−0.0030	−0.1229
C1	0.0519	−0.0935
C2	0.0905	−0.1686
D	0.0911	−0.2295
D	0.0911	−0.2295
C3	0.1275	−0.0846
D	0.1269	−0.0237
D	0.1269	−0.0237
C4	0.1662	−0.1597
D	0.1668	−0.2206
D	0.1668	−0.2206
C5	0.2032	−0.0757
D	0.2026	−0.0148
D	0.2026	−0.0148
C6	0.2419	−0.1508
D	0.2425	−0.2117
D	0.2425	−0.2117
C7	0.2789	−0.0668
D	0.2783	−0.0059
D	0.2783	−0.0059
C8	0.3176	−0.1419
D	0.3182	−0.2028
D	0.3182	−0.2028
C9	0.3546	−0.0579
D	0.3539	0.0030
D	0.3539	0.0030
C10	0.3932	−0.1330
D	0.3939	−0.1939
D	0.3939	−0.1939
C11	0.4303	−0.0490
D	0.4296	0.0119
D	0.4296	0.0119
D	0.4563	−0.1069

All of the acids with an odd number of carbon atoms in the chain can be indexed on a rectangular unit cell of plane group pgg containing 4 molecules. In contrast, those members of the series with even numbers of carbons atoms show a number of "split" reflections and can only be indexed on oblique unit cells.

Calculations indicate that the experimental patterns are not particularly sensitive to the rotation of the molecules about their long axes. The best fit is found for molecules that have the carbon backbone parallel to the graphite with a precision of approximately ±30°. The molecular orientation in all of the odd monolayers was found to be essentially parallel to the *a*-direction of the unit cell, with an uncertainty of approximately 3°.

The relative positions of the species in the hydrogen bond have been investigated, and the intermolecular arrangement of the two acid groups that form the hydrogen bond was refined. It was found that the molecular arrangement of the hydrogen bond in the fitted structures cannot be distinguished from the bulk within the resolution of our data. The energies of dimerization through hydrogen bonding in bulk acids[35] is approximately 60 kJ mol^{-1}, and the typical van der Waals interaction energies for the molecules in adsorbed layers are reflected in the melting enthalpies of alkanes,[36] typically 7 kJ mol^{-1}. Hence, we would expect the much stronger hydrogen bond to form its preferred geometry, as observed. Indeed, recent evidence has indicated that the acid molecules retain their dimeric form on melting in the monolayer.[37]

There is an additional weak feature at $q = 8.3$ nm^{-1} in the neutron pattern in Figure 2a for hexanoic and tridecanoic acids at low coverage. There is no evidence for this peak in the X-ray patterns or the high coverage neutron pattern of tridecanoic acid. The rest of the hexanoic and tridecanoic fits are reasonable, with isomorphic structures that fit all of the other X-ray and neutron patterns. Based on these factors, our present assessment is that this feature is an artifact. We suspect that small relative shifts in the (0,2) peaks for heptanoic acid in the X-ray and neutron patterns may arise from small differences in coverage and temperature. However, we cannot exclude the possibility of larger and more complex structures that are beyond the resolution and number of available peaks in the current data.

It is noted that all of the even and odd monolayer structures are closely related. The break in symmetry of those members with even numbers of carbons atoms is slight and may reflect subtle differences in packing of the ends of the chains. The dimerized pairs of molecules are essentially linear with a "step" or "kink" in the middle where the acid headgroups are. In the odd homologoues, these "kinks" alternate in direction, resulting in a rectangular unit cell after two dimers. In the even homologues, every kink goes the same way, resulting in an oblique unit cell. This behavior has been reported previously in the odd−even variations seen in the bulk material where packing of the chains is reported to lead to different space groups for odd and even homologues[22] and in STM images of the longer homologues adsorbed from solution.[16]

Interestingly, the dimensions of the monolayers resemble those of certain planes of the bulk crystal lattices. However, the molecular positions in the unit cell do not appear to be the same as those in the bulk (specific calculations of the X-ray and neutron scattering patterns from bulk planes show significant differences to the experimental data). Particularly, the molecules in the monolayer are interdigitated unlike the bulk, Figure 1. Usually such a similarity in lattice parameters would be taken as some indication that bulk crystals could grow from the surface, as there would be little lattice strain energy.[1,2] However, the differences in molecular positions in the unit cells observed here between the bulk and the surface suggest that these carboxylic acids would not be expected to grow in such a layer-by-layer fashion. Previous work by Findenegg also appears to support this tentative conclusion:[9] adsorbed alcohols show evidence of multilayer formation close to the bulk melting point, and adsorbed carboxylic acids do not show such behavior. In addition, in our extensive calorimetric studies of adsorbed acids we do not see "layering transitions" for adsorbed acids that are observed for many adsorbed alcohols.

The isomorphism of all of the solid monolayers also provides some comfort in the structural solutions we have presented, as it is very unlikely that such similar structures would fit all of

the experimental data, both X-rays and neutrons, if these had not been the correct structures. However, given that a larger unit cell with more degrees of freedom could always fit the observed data as well as the structures presented here larger, more complex structures cannot be ruled out.

Discussion and Summary

The low-temperature submonolayer and higher multilayer coverage structures of the linear carboxylic acids, hexanoic to tetradecanoic, have been reported. The odd members have a rectangular unit cell with plane group pgg and contain 4 molecules. In contrast, the members with an even number of carbon atoms have a slightly oblique unit cell with two molecules and plane group p2. The molecules in all of the structures have the planes of their carbon backbones essentially parallel to the graphite. The crystallographic structure of all monolayers has pgg or p2 symmetry, in agreement with the close-packing predictions of Kitaigorodskii,[33] for dimers of molecules with c2 or a center of inversion symmetry. Interestingly, this close packing is apparently achieved even in the presence of strong hydrogen bonds.

The slightly different symmetries and structures identified here for odd and even homologues provide a structural origin for the observed odd−even variation in monolayer melting points reported previously.[37] The similarities between the molecular packing in the odd and even unit cells also provide an explanation for the good mixing observed in mixed acid monolayers.[37]

The STM images[16] from heptadecanoic acid (C_{17}) and nonandecanoic acid (C_{19}) adsorbed on graphite from phenyl octane solution have been interpreted as a rectangular unit cell with four molecules with the pgg plane group, which is isomorphic with that we have deduced for all of the shorter odd members of the homologous series we have investigated. Hence, there is good agreement between the structures deduced by STM and these diffraction measurements.

We can quantitatively compare our monolayer structure for myristic acid (C_{14}) with that determined by STM[17] adsorbed from phenyloctane on graphite. The STM image has been interpreted as a unit cell, with two dimerized molecules in a similar interdigitated molecular arrangement that we have deduced, with a similar slightly oblique unit cell. Although the STM unit cell parameters are not given, the molecular length is reported as 2.01 ± 0.38 nm and the distance between the alkyl chains is 0.50 ± 0.03 nm. These compare very well with the equivalent dimensions reported here. The dimension parallel to the molecular axis (2.02 ± 0.01 nm) and the "*b*" parameter is twice the molecular separation (0.962 ± 0.002 nm). We conclude that the structures determined by STM for the longer acid homologues adsorbed on graphite from solution are in good agreement with those determined here using X-ray and neutron diffraction for the shorter homologues.

Diffraction experiments have demonstrated that monolayers of even membered shorter alkanes (<C12) exhibit monolayer structures different from the longer and odd members of the series.[5,6,26,38] Interestingly, we conclude that odd and even saturated acid monolayers have different structures but that the shorter homologues are similar in structure to the longer ones (down to at least C_6).

These structures provide insight into the delicate interplay of interactions within the layer and between the layer and the surface. The monolayer structure consists of interdigitated dimers, with a different packing from bulk planes. The interdigitation may arise to maximize oxygen−oxygen distances, as the molecules cannot twist on graphite as they do in the bulk. The acid headgroup configuration is the same as the bulk, demonstrating that the physisorption energy is strong enough to perturb the van der Waals intermolecular bonding, but not the hydrogen bonding.

Acknowledgment. We thank UK EPSRC and Unilever PLC (A.K.B.), The Leverhulme Trust (L.M.), BP (A.P.), and JSPS (Grant No. A-16205001) (A.I.) for financial support, and the staff and scientists at the ILL and ISIS for beam time and technical assistance.

References and Notes

(1) Muirhead, R. J.; Dash, J. G.; Krim, J. *Phys. Rev.* **1984**, *B29*, 5074.
(2) Seguin, J. L.; Suzanne, J.; Bianfait, M.; Dash, J. G.; Venables, J. A. *Phys. Rev. Lett.* **1983**, *51*, 122.
(3) Messe, L.; Perdigon, A.; Clarke, S. M.; Inaba, A.; Castro, M. A. *J. Colloid Interface Sci.* **2002**, *266*, 19.
(4) Clarke, S. M.; Messe, L.; Adams, J.; Inaba, A.; Arnold, T.; Thomas, R. K. *Chem. Phys. Lett.* **2003**, *373*, 480.
(5) Arnold, T.; Dong, C. C.; Thomas, R. K.; Castro, M. A.; Perdigon, A.; Clarke, S. M.; Inaba, A. *Phys. Chem. Chem. Phys.* **2002**, *4*, 3430.
(6) Arnold, T.; Thomas, R. K.; Castro, M. A.; Clarke, S. M.; Messe, L.; Inaba, A. *Phys. Chem. Chem. Phys.* **2002**, *4*, 345.
(7) Duffy, D. C.; Friedmann, A.; Boggis, S. A.; Klenerman, D. *Langmuir* **1998**, *14*, 6518.
(8) Findenegg, G. H. *J. Chem. Soc., Faraday Trans I* **1972**, *168*, 1799.
(9) Findenegg, G. H. *J. Chem. Soc., Faraday Trans.* **1973**, *169*, 1069.
(10) Epseau, P.; Reynolds, P. A.; Dowling, T.; Cookson, D.; White, J. *J. Chem. Soc., Faraday Trans.* **1997**, *93*, 3201.
(11) Epseau, P.; White, J. *J. Chem. Soc., Faraday Trans.* **1997**, *93*, 3197.
(12) Morishige, K.; Kato, T. *J. Chem. Phys.* **1999**, *111*, 7095.
(13) Morishige, K.; Sakamoto, Y. *J. Chem. Phys.* **1995**, *103*, 2354.
(14) Morishige, K.; Takami, Y.; Yokota, Y. *Phys. Rev.* **1993**, *B48*, 8277.
(15) Giancarlo, L. C.; Flynn, G. W. *Annu. Rev. Phys. Chem.* **1998**, *49*, 297.
(16) Hibino, M.; Sumi, A.; Tsuchiya, H.; Hatta, I. *J. Phys. Chem.* **1998**, *B102*, 4544.
(17) Hibino, M.; Sumi, A.; Hatta, I. *Jpn. J. Appl. Phys.* **1995**, *34*, 3354.
(18) Hatta, I.; Nishino, J.; Sumi, A.; Hibino, M. *Jpn. J. Appl. Phys.* **1995**, *34*, 3930.
(19) Kuroda, R.; Kishi, E.; Yamano, A.; Hatanaka, K.; Matsuda, H.; Eguchi, K.; Nakagiri, T. *J. Vac. Sci. Technol.* **1991**, *B9*, 1180.
(20) Kishi, E.; Matusda, H.; Kuroda, R.; Takimoto, K.; Yamano, A.; Eguchi, K.; Hatanaka, K.; Nakagiri, T. *Ultramicroscopy* **1992**, *42*−*44*, 1067.
(21) Rabe, J. P.; Buchholz, S. *Science* **1991**, *253*, 424.
(22) Bond, A. D. *New J. Chem.* **2004**, *28*, 104.
(23) Camillone, N., III; Leung, T. Y. B.; Schwartz, P.; Eisenberger, P.; Scoles, G. *Langmuir* **1996**, *12*, 2737.
(24) Poirier, G. E. *Langmuir* **1999**, *15*, 1167.
(25) Schwartz, P. V.; Lavrich, D. J.; Scoles, G. *Langmuir* **2003**, *19*, 4969.
(26) Herwig, K. W.; Matthies, B.; Taub, H. *Phys. Rev. Lett.* **1995**, *75*, 3154.
(27) Venkataraman, B.; Breen, J. J.; Flynn, G. W. *J. Phys. Chem.* **1995**, *99*, 6608.
(28) Wintgens, D.; Yablon, D. G.; Flynn, G. W. *J. Phys. Chem. B* **2003**, *107*, 173.
(29) ILL. "Neutron Research Facilities at the ILL High Flux Reactor", Institut Laue-Langevin, 1996.
(30) Inaba, A.; Clarke, S. M.; Arnold, T.; Thomas, R. K. *Chem. Phys. Lett.* **2002**, *352*, 57.
(31) Kjems, J. K.; Passell, L.; Taub, H.; Dash, J. G.; Novaco, A. D. *Phys. Rev.* **1976**, *B13*, 1446.
(32) Warren, B. E. *Phys. Rev.* **1941**, *59*, 693.
(33) Clarke, S. M.; Thomas, R. K. *Mol. Phys.* **1991**, *72*, 413.
(34) Groszek, A. J. *Proc. R. Soc. London* **1970**, *A314*, 473.
(35) Emmeluth, C.; Suhm, M. A. *Phys. Chem. Chem. Phys.* **2003**, *5*, 3094.
(36) Messe, L.; Perdigon, A.; Clarke, S. M.; Inaba, A.; Arnold, T. *Langmuir* **2005**, *21*, 5085.
(37) Bickerstaffe, A. K.; Messe, L.; Clarke, S. M.; Parker, J.; Perdigon, A.; Cheah, N. P.; Inaba, A. *Phys. Chem. Chem. Phys.* **2004**, *6*, 3545.
(38) Herwig, K. W.; Newton, J. C.; Taub, H. *Phys. Rev. B* **1994**, *50*, 15287.